Slawomir Koziel
Leifur Leifsson *Editors*

Surrogate-Based Modeling and Optimization

Applications in Engineering

Springer

Surrogate-Based Modeling and Optimization

Slawomir Koziel • Leifur Leifsson
Editors

Surrogate-Based Modeling and Optimization

Applications in Engineering

Springer

Editors
Slawomir Koziel
Engineering Optimization & Modeling Cent
Reykjavik University
Reykjavik, Iceland

Leifur Leifsson
School of Science and Engineering,
Engineering Optimization & Modeling
Reykjavik University
Reykjavik, Iceland

ISBN 978-1-4614-7550-7 ISBN 978-1-4614-7551-4 (eBook)
DOI 10.1007/978-1-4614-7551-4
Springer New York Heidelberg Dordrecht London

Library of Congress Control Number: 2013941933

Mathematics Subject Classification (2010): 74P10, 80M50, 97M10, 62P30

Printed on acid-free paper

Springer is part of Springer Science+Business Media (www.springer.com)

Preface

Contemporary engineering design is heavily based on computer simulations. Accurate, high-fidelity simulations are used not only for design verification but, most importantly, to adjust parameters of the system (e.g., wing geometry, material parameters of antennas) so that it meets given performance requirements. Unfortunately, accurate simulations are often computationally expensive, with evaluation times ranging from hours to days per design. Consequently, design automation using conventional optimization methods is often impractical or even prohibitive. Other issues include the numerical noise that is often present in simulation responses, and the absence of sensitivity information. These, and other problems, can be alleviated by the development and employment of so-called surrogates, which reliably represent the expensive, simulation-based model of the system/device of interest, but are much cheaper and analytically tractable.

This edited book is about surrogate-based modeling and optimization techniques and their applications for solving difficult and computationally expensive engineering design problems. A group of international experts summarize recent developments in the field and demonstrate applications in various disciplines of engineering and science. The main purpose of the work is to provide the basic concepts and formulations of the surrogate-based modeling and optimization paradigm, as well as to discuss relevant modeling techniques, optimization algorithms, and design procedures.

Simulation-driven design based on surrogate models plays an increasingly important role in contemporary engineering and permits us to solve problems that cannot be solved otherwise, particularly by dramatically reducing the computational cost of the solution process. Unfortunately, recent results concerning surrogate-based modeling and optimization are scattered throughout the literature in various engineering fields and, therefore, are not easily accessible to a reader interested in this technology. Thus, this book should be of interest to engineers from any discipline where computationally heavy simulations (such as finite element, computational fluid dynamics, and computational electromagnetics analyses) are used on a daily basis in the design process. The editors of this volume hope that the presented material will allow the readers to gain an understanding of the basic mechanisms of the surro-

gate modeling process and familiarize themselves with important components of surrogate-based optimization algorithms and the advantages of employing variable-fidelity simulation-driven design, as well as enable them to reduce the cost of the design process aided by computer simulations.

Reykjavik, Iceland
March 2013

Slawomir Koziel
Leifur Leifsson

Contents

Space Mapping for Electromagnetic-Simulation-Driven Design Optimization

Slawomir Koziel, Leifur Leifsson, and Stanislav Ogurtsov

Abstract Space mapping (SM) has been one of the most popular surrogate-based optimization techniques in microwave engineering to date. By exploiting the knowledge embedded in the underlying coarse model (e.g., an equivalent circuit), SM allows dramatic reduction of the computational cost while optimizing electromagnetic (EM)-simulated structures such as filters or antennas. While potentially very efficient, SM is not always straightforward to implement and set up, and may suffer from convergence problems. In this chapter, we discuss several variations of an SM optimization algorithm aimed at improving SM performance for design problems involving EM simulations. These include SM with constrained parameter extraction and surrogate model optimization designed to overcome the problem of selecting preassigned parameters for implicit SM, SM with response surface approximation coarse models that maintain SM efficiency when a fast coarse model is not available, and SM with sensitivity which takes advantage of adjoint sensitivity (which has recently become commercially available in EM simulators) to improve the convergence properties and further reduce the computational cost of SM algorithms. Each variation of the SM algorithm presented here is illustrated using a real-world microwave design example.

Keywords Computer-aided design (CAD) · Microwave engineering · Simulation-driven optimization · Electromagnetic (EM) simulation · Surrogate-based optimization · Space mapping · Surrogate model · High-fidelity model · Coarse model

1 Introduction

Space mapping (SM) [1–3] was originally developed in the 1990s to deal with computationally expensive design problems in microwave engineering [3, 4]. Automated design closure of structures evaluated using electromagnetic (EM) simu-

S. Koziel (✉) · L. Leifsson · S. Ogurtsov
Engineering Optimization & Modeling Center, School of Science and Engineering, Reykjavik University, Menntavegur 1, 101 Reykjavik, Iceland
e-mail: koziel@ru.is

S. Koziel, L. Leifsson (eds.), *Surrogate-Based Modeling and Optimization*,
DOI 10.1007/978-1-4614-7551-4_1,

lations is still a challenging task today, mostly due to the high computational cost of accurate, high-fidelity EM simulation. The presence of massive computing resources does not always translate into computational speedup. This is due to a growing demand for simulation accuracy (which requires, among other things, finer discretization of the structure), as well as the necessity of including important interactions between the structure under design and its environment (e.g., antenna housing and connectors, etc.), which increases the computational domain and, consequently, slows down the simulation. At the same time, multiphysics simulations (e.g., including thermal effects) become more and more important, further contributing to the computational cost of the simulation. As conventional optimization algorithms (e.g., gradient-based schemes with numerical derivatives) require tens, hundreds, or even thousands of objective function calls per run (depending on the number of design variables), the computational cost of the whole optimization process may not be acceptable.

SM belongs to a broader family of methods called surrogate-based optimization (SBO) techniques [5–7]. SM and most other SBO methods share a main structure, in which the direct optimization of the expensive (here, EM-simulated) structure, referred to as the high-fidelity or fine model, is replaced by iterative refinement and reoptimization of a low-fidelity (or coarse) model. The coarse model is a physics-based representation of the high-fidelity one. It is less accurate but supposedly much faster than the latter. An example of a coarse model in microwave engineering is an equivalent circuit which describes the same structure as the fine model but using circuit theory rather than full-wave EM simulation. The SM surrogate is constructed by enhancing the coarse model through auxiliary transformations, usually linear, with parameters of these transformations obtained in what is called the parameter extraction (PE) process [8], which is a trademark of SM. PE is executed to reduce the misalignment between the responses of the space-mapped coarse model and the fine model at a limited number of designs, usually those that have already emerged during the SM optimization run. The benefit of SM lies in the fact that each SM iteration usually requires evaluation the high-fidelity model at a single design (the one obtained by optimizing the current surrogate model), and—for a well-performing algorithm—only a few iterations are necessary to yield a satisfactory design.

SM has been successfully applied to optimize a number of microwave components, the majority of which are filters [1–4] and impedance transformers [8], but also antennas [9–11], etc. As mentioned before, one of the fundamental prerequisites of SM is that the underlying coarse model be fast, so that the computational overhead related to parameter extraction and surrogate model optimization performed at each iteration of the algorithm can be neglected. For this reason, equivalent circuit models are preferred. Unfortunately, reliable equivalent circuit models are not available for many structures, including broadband antennas [12] and substrate integrated structures [13]. Also, if EM coupling between the device of interest and its environment has to be taken into account (e.g., an antenna mounted in a cellphone or on a vehicle), full-wave simulation is probably the only way to evaluate the system. A possible lack of fast models poses a difficulty for SM, because the computational overhead related to multiple evaluation of the low-fidelity model, particularly due to PE, may determine the total CPU cost of the SM process.

Another issue is convergence: as SM does not use sensitivity information by default, it is not globally convergent in a conventional sense, unless certain conditions regarding similarity between the low- and high-fidelity models [14] are met. Those conditions are, unfortunately, difficult to verify in practice [15]. At the same time, SM offers a number of ways of constructing the surrogate model. A number of elementary transformations (input SM [8], implicit SM [16], or frequency SM [2, 14]) can be combined into more involved models. The specific choice of the model affects the algorithm performance [17], and the optimal choice is not trivial [15].

In this chapter, we discuss several variations of the SM algorithms specifically targeted at improving the SM performance for microwave engineering applications. The chapter is organized as follows. In Sect. 2, we recall the SM concept and formulate a generic SM algorithm. In Sect. 3, we describe implicit SM with constrained parameter extraction, which helps improve convergence of the SM algorithm without requiring careful selection of its preassigned parameters. Section 4 is devoted to SM with auxiliary response surface approximation coarse models. This approach aims at improving the efficiency of the SM optimization process in situations when the available low-fidelity models are relatively expensive (e.g., obtained through coarse-discretization EM simulations), which is usually the case in antenna design. In Sect. 5, we discuss the enhancement of SM using adjoint sensitivity. By exploiting derivative information whenever possible, specifically, to enhance the surrogate model as well as to speed up both PE and surrogate model optimization, it is possible to improve the algorithm convergence and to reduce its computational cost. Section 6 concludes the chapter with some recommendations for readers interested in applying SM in their design work.

2 Space Mapping Optimization: A Brief Introduction

In this section, we briefly recall the formulation of the generic space mapping (SM) algorithm, the concept of parameter extraction (PE), and the basic types of SM surrogate models.

A microwave design task can be formulated as a nonlinear minimization problem

$$\boldsymbol{x}^* \in \arg\min_{\boldsymbol{x} \in X_f} U\left(\boldsymbol{R}_f(\boldsymbol{x})\right), \tag{1}$$

where $\boldsymbol{R}_f \in R^m$ denotes the response vector of the device of interest, e.g., the modulus of the transmission coefficient $|S_{21}|$ evaluated at m different frequencies. U is a given scalar merit function, e.g., a minimax function with upper and lower specifications [8]. Vector $\boldsymbol{x}^*$ is the optimal design to be determined. Normally, $\boldsymbol{R}_f$ is obtained through computationally expensive electromagnetic (EM) simulation, and is referred to as the high-fidelity or fine model. Because of the high computational cost, using conventional optimization techniques to handle (1) may be impractical; both gradient-based (e.g., quasi-Newton [18]) and derivative-free (pattern search [19], genetic algorithms [20]) methods usually require a substantial number of objective function (and thus, high-fidelity model) evaluations.

SM [1–3, 21] is a methodology that aims at reducing the cost of solving the problem (1). SM belongs to a broader class of surrogate-based optimization (SBO) techniques [7–9]. Similarly to other SBO methods, SM speeds up the design process by shifting the optimization burden to an inexpensive yet reasonably accurate surrogate model of the device of interest. In the generic SM framework described here the direct optimization of the computationally expensive EM-simulated high-fidelity model $\boldsymbol{R}_f$ is replaced by an iterative procedure [7, 14]

$$\boldsymbol{x}^{(i+1)} = \arg\min_{\boldsymbol{x}} U\left(\boldsymbol{R}_s^{(i)}(\boldsymbol{x})\right), \tag{2}$$

that generates a sequence of points (designs) $\boldsymbol{x}^{(i)} \in X_f$, $i = 0, 1, \ldots$, that are approximate solutions to the original design problem (1). Each $\boldsymbol{x}^{(i+1)}$ is the optimal design of the surrogate model $\boldsymbol{R}_s^{(i)} : X_s^{(i)} \to R^m$, $X_s^{(i)} \subseteq R^n$, $i = 0, 1, \ldots$. $\boldsymbol{R}_s^{(i)}$ is assumed to be a computationally cheap and sufficiently reliable representation of the fine model $\boldsymbol{R}_f$, particularly in the neighborhood of the current design $\boldsymbol{x}^{(i)}$. Under these assumptions, the algorithm (2) is likely to produce a sequence of designs that quickly approach $\boldsymbol{x}_f^*$.

Typically, $\boldsymbol{R}_f$ is only evaluated once per iteration (at every new design $\boldsymbol{x}^{(i+1)}$) for verification purposes and to obtain the data necessary to update the surrogate model. Since the surrogate model is computationally cheap, its optimization cost (cf. (2)) can usually be neglected, and the total optimization cost is determined by the evaluation of $\boldsymbol{R}_f$. The key point here is that the number of evaluations of $\boldsymbol{R}_f$ for a well-performing surrogate-based algorithm is substantially smaller than for any direct optimization method (e.g., a gradient-based one). Figure 1 shows the block diagram of the SM optimization process.

If the surrogate model satisfies zero- and first-order consistency conditions with the fine model, i.e., $\boldsymbol{R}_s^{(i)}(\boldsymbol{x}^{(i)}) = \boldsymbol{R}_f(\boldsymbol{x}^{(i)})$ and $(\partial \boldsymbol{R}_s^{(i)}/\partial \boldsymbol{x})(\boldsymbol{x}^{(i)}) = (\partial \boldsymbol{R}_f/\partial \boldsymbol{x})(\boldsymbol{x}^{(i)})$ (verification of the latter requires $\boldsymbol{R}_f$ sensitivity data), and the algorithm (2) is enhanced by the trust region method [22], then it is provably convergent to a local fine model optimum [23]. Convergence can also be guaranteed if the algorithm (2) is enhanced by properly selected local search methods [24]. SM [8, 14, 25, 26] does not normally rely on the aforementioned enhancements; however, it requires the surrogate model to be constructed from the physically based coarse model [8]. This usually gives remarkably good performance in the sense of the SM algorithm being able to quickly locate a satisfactory design.

The way that SM constructs the surrogate model for the iterative process (2) is one of the features that distinguish this technique from many other SBO approaches. The surrogate model at iteration i, $\boldsymbol{R}_s^{(i)}$, is constructed from the low-fidelity model so that the misalignment between $\boldsymbol{R}_s^{(i)}$ and the fine model is minimized using the parameter extraction (PE) process, which is the nonlinear minimization problem by itself [8]. The surrogate is defined as [14]

$$\boldsymbol{R}_s^{(i)}(\boldsymbol{x}) = \boldsymbol{R}_{s.g}\left(\boldsymbol{x}, \boldsymbol{p}^{(i)}\right), \tag{3}$$

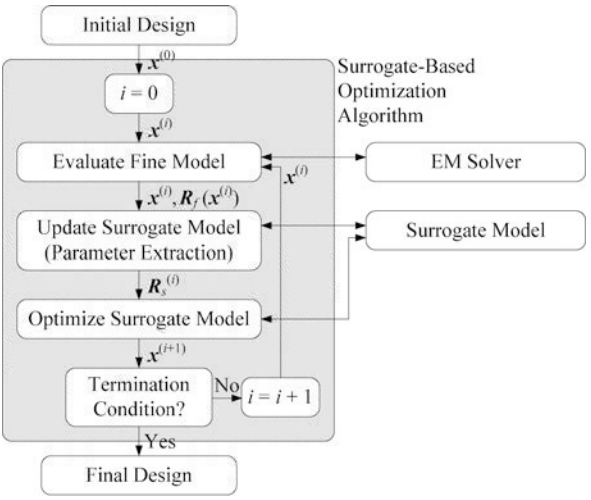

Fig. 1 Surrogate-based simulation-driven design optimization: the optimization burden is shifted to the computationally cheap surrogate model which is updated and reoptimized at each iteration of the main optimization loop. High-fidelity EM simulation is only performed once per iteration to verify the design produced by the surrogate model and to update the surrogate itself. The number of iterations for a well-performing SBO algorithm is substantially smaller than for conventional techniques

where $\boldsymbol{R}_{s.g}$ is a generic SM surrogate model, i.e., the low-fidelity model composed with suitable transformations, whereas

$$\boldsymbol{p}^{(i)} = \arg\min_{\boldsymbol{p}} \sum_{k=0}^{i} w_{i.k} \left\| \boldsymbol{R}_f\left(\boldsymbol{x}^{(k)}\right) - \boldsymbol{R}_{s.g}\left(\boldsymbol{x}^{(k)}, \boldsymbol{p}\right) \right\| \tag{4}$$

is a vector of model parameters and $w_{i.k}$ are weighting factors; a common choice of $w_{i.k}$ is $w_{i.k} = 1$ for all i and all k.

Various SM surrogate models are available [8, 14]. They can be roughly categorized into four groups:

- Models based on a (usually linear) distortion of coarse model parameter space, e.g., input SM of the form $\boldsymbol{R}_{s.g}(\boldsymbol{x}, \boldsymbol{p}) = \boldsymbol{R}_{s.g}(\boldsymbol{x}, \boldsymbol{B}, \boldsymbol{c}) = \boldsymbol{R}_c(\boldsymbol{B} \cdot \boldsymbol{x} + \boldsymbol{c})$ [8];
- Models based on a distortion of the coarse model response, e.g., output SM of the form $\boldsymbol{R}_{s.g}(\boldsymbol{x}, \boldsymbol{p}) = \boldsymbol{R}_{s.g}(\boldsymbol{x}, \boldsymbol{d}) = \boldsymbol{R}_c(\boldsymbol{x}) + \boldsymbol{d}$ [14];
- Implicit SM, where the parameters used to align the surrogate with the fine model are separate from the design variables, i.e., $\boldsymbol{R}_{s.g}(\boldsymbol{x}, \boldsymbol{p}) = \boldsymbol{R}_{s.g}(\boldsymbol{x}, \boldsymbol{x}_p) = \boldsymbol{R}_{c.i}(\boldsymbol{x}, \boldsymbol{x}_p)$, with $\boldsymbol{R}_{c.i}$ being the coarse model dependent on both the design variables $\boldsymbol{x}$ and the preassigned parameters $\boldsymbol{x}_p$ (e.g., dielectric constant, substrate height) that are normally fixed in the fine model but can be freely altered in the coarse model [14];
- Custom models exploiting parameters characteristic to a given design problem; the most characteristic example is frequency SM $\boldsymbol{R}_{s.g}(\boldsymbol{x}, \boldsymbol{p}) = \boldsymbol{R}_{s.g}(\boldsymbol{x}, \boldsymbol{F}) =$

$\boldsymbol{R}_{c.f}(\boldsymbol{x}, \boldsymbol{F})$ [8], where $\boldsymbol{R}_{c.f}$ is a frequency-mapped coarse model, i.e., the coarse model evaluated at frequencies ω different from the original frequency sweep for the fine model, according to the mapping $\omega \rightarrow f_1 + f_2\omega$, with $\boldsymbol{F} = [f_1\, f_2]^T$.

SM usually comprises combined transformations. For instance, a surrogate model employing input, output, and frequency SM transformations would be $\boldsymbol{R}_{s.g}(\boldsymbol{x}, \boldsymbol{p}) = \boldsymbol{R}_{s.g}(\boldsymbol{x}, \boldsymbol{c}, \boldsymbol{d}, \boldsymbol{F}) = \boldsymbol{R}_{c.f}(\boldsymbol{x} + \boldsymbol{c}, \boldsymbol{F}) + \boldsymbol{d}$. The rationale for this is that a properly chosen mapping may significantly improve the performance of the SM algorithm; however, the optimal selection of the mapping type for a given design problem is not trivial [15]. Work has been done to ease the selection process for a given design problem [17, 27]. However, regardless of the mapping choice, coarse model accuracy is what principally affects the performance of the SM design process. One can quantify the quality of the surrogate model through rigorous convergence conditions [15]. These conditions, although useful for developing more efficient SM algorithms and automatic surrogate model selection techniques, cannot usually be verified because of the limited amount of data available from the fine model. In practice, the most important criterion for assessing the quality or accuracy of the coarse model is still visual inspection of the fine and coarse model responses at certain points and/or examining absolute error measures such as $\|\boldsymbol{R}_f(\boldsymbol{x}) - \boldsymbol{R}_c(\boldsymbol{x})\|$.

The coarse model is the most important factor that affects the performance of the SM algorithm. The first stems from accuracy. Coarse model accuracy (more generally, the accuracy of the SM surrogate [15]) is the main factor that determines the efficiency of the algorithm in terms of finding a satisfactory design. The more accurate the coarse model, the smaller the number of fine model evaluations necessary to complete the optimization process. If the coarse model is insufficiently accurate, the SM algorithm may need more fine model evaluations or may even fail to find a good quality design.

The second important characteristic is the evaluation cost. It is essential that the coarse model be computationally much cheaper than the fine model, because both PE (4) and surrogate optimization (2) require large numbers of coarse model evaluations. Ideally, the evaluation cost of the coarse model should be negligible when compared to the evaluation cost of the fine model, in which case the total computational cost of the SM optimization process is merely determined by the necessary number of fine model evaluations. If the evaluation time of the coarse model is too high, say, larger than 1 % of the fine model evaluation time, the computational cost of surrogate model optimization and, especially, PE, start playing important roles in the total cost of SM optimization and may even determine it. Therefore, practical applicability of SM is limited to situations where the coarse model is computationally much cheaper than the fine model. The majority of SM models reported in the literature (e.g., [4, 8, 14]) concern microstrip filters, transformers, or junctions where fast and reliable equivalent circuit coarse models are easily available.

3 Implicit Space Mapping with Constrained Parameter Extraction for Microwave Filter Design

In this section, we discuss SM with constrained PE [28] as a way to alleviate the problems related to the proper selection of the SM parameters used to construct the surrogate model as well as to improve convergence properties of the SM algorithm. Without loss of generality, we restrict our considerations to implicit SM [16], the most general approach to SM. Implicit SM allows us to introduce any number of surrogate model parameters. In particular, over-flexibility of the surrogate model required by our method can be easily obtained. Also, implicit SM can incorporate most other SM types, including input and output SM.

3.1 Implicit Space Mapping Algorithm

Implicit SM follows the generic SM scheme (2); however, for better clarity, we assume here a specific form of the SM surrogate model. Let $\boldsymbol{R}_c : X_c \times X_p \to R^m, \in R^m$ denote the response vector of the coarse model that describes the same object as the fine model: less accurate but much faster to evaluate. $\boldsymbol{R}_c$ depends on two sets of parameters: (i) design variables $\boldsymbol{x}$, the same as in the fine model, and (ii) preassigned parameters $\boldsymbol{x}_p$, i.e., parameters that are normally fixed in the fine model (e.g., dielectric constants) but can be adjusted in the coarse model to match it to $\boldsymbol{R}_f$.

The generic SM algorithm (2) can then be reformulated as follows:

$$\boldsymbol{x}^{(i+1)} = \arg\min_{\boldsymbol{x}} U\left(\boldsymbol{R}_c\left(\boldsymbol{x}, \boldsymbol{x}_p^{(i)}\right)\right), \tag{5}$$

where

$$\boldsymbol{x}_p^{(i)} = \arg\min_{\boldsymbol{x}_p} \left\| \boldsymbol{R}_f\left(\boldsymbol{x}^{(i)}\right) - \boldsymbol{R}_c\left(\boldsymbol{x}^{(i)}, \boldsymbol{x}_p\right) \right\|. \tag{6}$$

Thus, the coarse model with adjusted values of preassigned parameters becomes a surrogate model for the implicit SM algorithm. We note that other types of SM can also be reformulated in terms of implicit SM. For example, the surrogate model of the most popular input SM [14] is defined as $\boldsymbol{R}_s(\boldsymbol{x}) = \boldsymbol{R}_c(\boldsymbol{x} + \boldsymbol{c})$, where $\boldsymbol{c}$ is an $n \times 1$ vector of parameters. It can be formulated in implicit SM terms as $\boldsymbol{R}_{c.i}(\boldsymbol{x}, \boldsymbol{x}_p)$, where $\boldsymbol{R}_{c.i}$ is the implicit-SM-like coarse model defined as $\boldsymbol{R}_{c.i}(\boldsymbol{x}, \boldsymbol{x}_p) = \boldsymbol{R}_c(\boldsymbol{x} + \boldsymbol{x}_p)$. In particular, the same software implementation can be used to realize our algorithm for both implicit and input cases. Analogous reformulations can be defined for scaling-like input SM $\boldsymbol{R}_s(\boldsymbol{x}) = \boldsymbol{R}_c(\boldsymbol{B} \cdot \boldsymbol{x})$, where $\boldsymbol{B}$ is an $n \times n$ matrix of SM parameters, output [14] and frequency SM [14].

3.2 Space Mapping with Constrained Parameter Extraction

The performance of SM algorithms depends heavily on the quality of the coarse model utilized in the optimization process and the type of mapping involved in

creating the surrogate model [15]. For implicit SM, the number of possible ways of selecting preassigned parameters is virtually unlimited. However, it is not obvious how to select a set of parameters that might allow the surrogate to closely approximate the fine model and simultaneously have good generalization capability. A wrong choice of the parameter set may result in inadequate performance of the SM algorithm, including convergence issues, poor quality of the final design, and excessive computational cost [17].

Various ways of alleviating this problem have been proposed. They include adaptive SM algorithms [17] and assessment methodologies [15, 29]. Although useful in the selection of the surrogate model and its parameters, none of these techniques guarantees algorithm convergence and overall good performance. On the other hand, trust region enhanced SM algorithms ensure algorithm convergence but not always a sufficient quality of the final design, because in the case of inadequate improvement of the objective function [30], they force the algorithm to terminate. Also, the trust region approach increases the computational cost of the SM optimization process.

The technique described in this section controls the trade-off between the approximation and generalization capability of the surrogate model by properly restricting the parameter space of the model. Theoretical justification of the method can be found in [28].

It is assumed that the initial surrogate model, i.e., the coarse model without any constraints on its preassigned parameters, is able to approximate the fine model with sufficient accuracy. This accuracy can be measured at a given iteration point $\boldsymbol{x}^{(i)}$, using any suitable criteria, e.g., $\varepsilon^{(i)} = \|\boldsymbol{R}_f(\boldsymbol{x}^{(i)}) - \boldsymbol{R}_c(\boldsymbol{x}^{(i)}, \boldsymbol{x}_p^{(i)})\|_p$, where $\|\cdot\|_p$ determines the norm type (e.g., $\|\cdot\|_2$ for the Euclidean norm, or $\|\cdot\|_\infty$ for the maximum norm). We would like $\varepsilon^{(i)}$ to be small, $\varepsilon^{(i)} \leq \varepsilon_{\max}$, where $\varepsilon_{\max}$ is a user-defined threshold value, so that the surrogate model is a sufficiently good representation of $\boldsymbol{R}_f$.

It is normally feasible to build a surrogate model satisfying the above requirements. Because $\boldsymbol{R}_c$ is physically based, its response is similar to that of $\boldsymbol{R}_f$. An appropriate surrogate model can then be created by introducing a sufficient number of preassigned parameters, e.g., dielectric constants and substrate heights corresponding, if necessary, to individual components of the microwave structure in question. Even synthetic parameters can be used (i.e., parameters not corresponding to any physical parameter in $\boldsymbol{R}_f$ but used to increase model flexibility, e.g., a small capacitor introduced between coupled lines in the microstrip filter model). A rule of thumb is that the number of parameters should be larger than the number of design variables. If necessary, other SM transformations (e.g., input, frequency) can be incorporated (cf. Sect. 2).

According to the algorithm proposed in [31], the parameter extraction (PE) process (6) is replaced by the following constrained version:

$$\boldsymbol{x}_p^{(i)} = \arg \min_{\boldsymbol{l}^{(i)} \leq \boldsymbol{x}_p \leq \boldsymbol{u}^{(i)}} \left\| \boldsymbol{R}_f\left(\boldsymbol{x}^{(i)}\right) - \boldsymbol{R}_c\left(\boldsymbol{x}^{(i)}, \boldsymbol{x}_p\right) \right\|, \tag{7}$$

where $\boldsymbol{l}^{(i)}$ and $\boldsymbol{u}^{(i)}$ are lower and upper bounds for the preassigned parameters at iteration i. We assume here that $\boldsymbol{l}^{(i)} = \boldsymbol{x}_p^{(i-1)} - \boldsymbol{\delta}^{(i)}$ and $\boldsymbol{u}^{(i)} = \boldsymbol{x}_p^{(i-1)} + \boldsymbol{\delta}^{(i)}$, where

$\boldsymbol{x}_p^{(i-1)}$ is the vector of model parameters at iteration $i-1$ ($\boldsymbol{x}_p^{(0)}$ represents the initial values of the preassigned parameters), whereas $\boldsymbol{\delta}^{(i)}$ is a vector representing the parameter space size ($\boldsymbol{\delta}^{(0)}$ is a user-defined initial value).

At iteration i, the algorithm adjusts $\boldsymbol{l}^{(i)}$ and $\boldsymbol{u}^{(i)}$ and performs PE as follows ($\boldsymbol{\delta}^{(i)}$, $\boldsymbol{x}_p^{(i-1)}$ and $\varepsilon_{\max}$ are input arguments):

1. Calculate $\boldsymbol{l}^{(i)} = \boldsymbol{x}_p^{(i-1)} - \boldsymbol{\delta}^{(i)}$ and $\boldsymbol{u}^{(i)} = \boldsymbol{x}_p^{(i-1)} + \boldsymbol{\delta}^{(i)}$;
2. Find $\boldsymbol{x}_p^{(i)}$ using (7);
3. If $\varepsilon^{(i)} \le \alpha_{\text{decr}} \cdot \varepsilon_{\max}$ then $\boldsymbol{\delta}^{(i+1)} = \boldsymbol{\delta}^{(i)} / \beta_{\text{decr}}$; Go to 6;
4. If $\varepsilon^{(i)} > \alpha_{\text{incr}} \cdot \varepsilon_{\max}$ then $\boldsymbol{\delta}^{(i+1)} = \boldsymbol{\delta}^{(i)} \cdot \beta_{\text{incr}}$; Go to 6;
5. Set $\boldsymbol{\delta}^{(i+1)} = \boldsymbol{\delta}^{(i)}$;
6. END;

Here, α_{decr}, α_{incr}, β_{decr}, and β_{incr} are user-defined parameters (typical values: $\alpha_{\text{decr}} = 1$, $\alpha_{\text{incr}} = 2$, $\beta_{\text{decr}} = 5$, $\beta_{\text{incr}} = 2$). Our algorithm tightens the PE constraints if the approximation error is sufficiently small; otherwise, it loosens them.

Note that constraint tightening improves the generalization capability of the surrogate model: the low approximation error $\varepsilon^{(i-1)} = \|\boldsymbol{R}_f(\boldsymbol{x}^{(i-1)}) - \boldsymbol{R}_c(\boldsymbol{x}^{(i-1)}, \boldsymbol{x}_p^{(i-1)})\|_p$ and $\varepsilon^{(i)} = \|\boldsymbol{R}_f(\boldsymbol{x}^{(i)}) - \boldsymbol{R}_c(\boldsymbol{x}^{(i)}, \boldsymbol{x}_p^{(i)})\|_p$ (satisfied when determining $\boldsymbol{x}_p^{(i-1)}$ and $\boldsymbol{x}_p^{(i)}$, respectively) makes it more likely to have $\|\boldsymbol{R}_f(\boldsymbol{x}^{(i-1)}) - \boldsymbol{R}_c(\boldsymbol{x}^{(i-1)}, \boldsymbol{x}_p^{(i)})\|_p$ small if $\boldsymbol{\delta}^{(i)}$ is reduced (because small $\|\boldsymbol{x}_p^{(i)} - \boldsymbol{x}_p^{(i-1)}\|_\infty \le \|\boldsymbol{\delta}^{(i)}\|_\infty$ implies the similarity of subsequent surrogate models).

The convergence properties of the SM algorithm can be explicitly controlled by constraining the surrogate optimization (2), which can be formulated as

$$\boldsymbol{x}^{(i+1)} = \arg \min_{\boldsymbol{x}, \|\boldsymbol{x} - \boldsymbol{x}^{(i)}\| \le \delta^{(i)}} U\left(\boldsymbol{R}_c\left(\boldsymbol{x}, \boldsymbol{x}_p^{(i)}\right)\right), \tag{8}$$

where $\delta^{(i)} = \alpha \cdot \|\boldsymbol{x}^{(i)} - \boldsymbol{x}^{(i-1)}\|$ with $\alpha < 1$ (recommended values are $\alpha = 0.6$ to 0.9; values too small could result in premature convergence without finding a satisfactory design). Note that (8) is mostly used as a safeguard, because good convergence should be ensured by the constrained PE algorithm formulated above. On the other hand, constrained surrogate optimization is useful in finding a new design in the close neighborhood of the current design $\boldsymbol{x}^{(i)}$ (an over-flexible surrogate model may result in many designs that are good with respect to specification error, but are not necessarily close to $\boldsymbol{x}^{(i)}$).

It should be emphasized that the procedure described here is not related to the trust region approach [22] that has been used to safeguard convergence for SM algorithms [30]. The latter reduces the search range for the surrogate model. It rejects a new design if it does not bring sufficient improvement with respect to the fine model specification [32]. This increases the computational cost of SM optimization. According to the algorithm described here, the new design is never rejected: the generalization of the surrogate model is accommodated by the adaptive PE procedure. As indicated in [28], the constrained PE algorithm is expected to improve the convergence of the SM algorithm. The details can be found in [28].

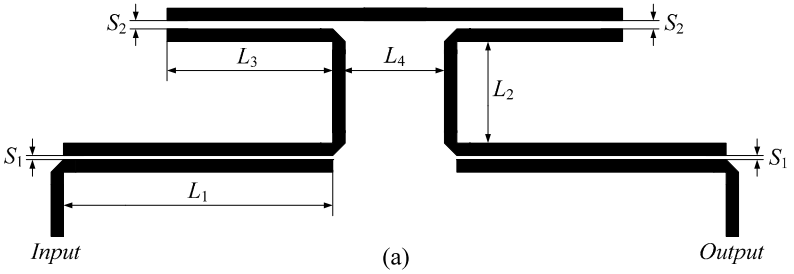

(a)

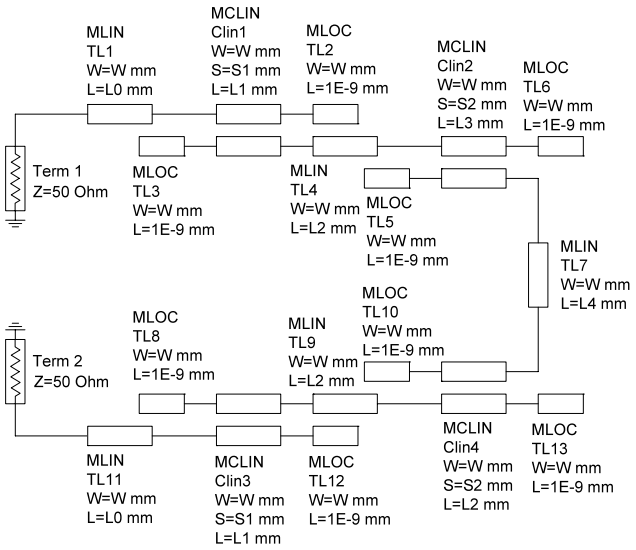

(b)

Fig. 2 Coupled microstrip bandpass filter: (**a**) geometry [33], (**b**) coarse model (Agilent ADS)

3.3 Design Example: Coupled Microstrip Bandpass Filter

Consider the coupled microstrip bandpass filter [33] shown in Fig. 2(a). The design parameters are $\boldsymbol{x} = [L_1\ L_2\ L_3\ L_4\ S_1\ S_2]^T$ mm. The fine model is simulated in FEKO [34]. The coarse model, Fig. 2(b), is an equivalent circuit implemented in Agilent ADS [35]. The design specifications are $|S_{21}| \geq -3$ dB for 2.3 GHz $\leq \omega \leq$ 2.5 GHz, and $|S_{21}| \leq -20$ dB for 1.8 GHz $\leq \omega \leq$ 2.15 GHz and 2.65 GHz $\leq \omega \leq$ 3.0 GHz. The initial design is $\boldsymbol{x}^{(0)} = [24\ 4\ 14\ 12\ 0.2\ 0.1]^T$ mm.

The SM surrogate model has 14 preassigned parameters: $\varepsilon_{r1} = \varepsilon_{r.\mathrm{Clin1}} = \varepsilon_{r.\mathrm{Clin3}}$, $\varepsilon_{r2} = \varepsilon_{r.\mathrm{TL4}} = \varepsilon_{r.\mathrm{TL9}}$, $\varepsilon_{r3} = \varepsilon_{r.\mathrm{Clin2}} = \varepsilon_{r.\mathrm{Clin4}}$, $\varepsilon_{r4} = \varepsilon_{r.\mathrm{TL7}}$, $H_1 = H_{\mathrm{Clin1}} = H_{\mathrm{Clin3}}$, $H_2 = H_{\mathrm{TL4}} = H_{\mathrm{TL9}}$, $H_3 = H_{\mathrm{Clin2}} = H_{\mathrm{Clin4}}$, $H_4 = H_{\mathrm{TL7}}$, and dL_1, dL_2, dL_3, dL_4, dS_1, dS_2 (design variable perturbations). Thus, we have $\boldsymbol{x}_p = [\varepsilon_{r1}\ \varepsilon_{r2}\ \varepsilon_{r3}\ \varepsilon_{r4}\ H_1\ H_2\ H_3\ H_4\ dL_1\ dL_2\ dL_3\ dL_4\ dS_1\ dS_2]^T$. Symbols $\varepsilon_{r.\mathrm{Elem}}$ and

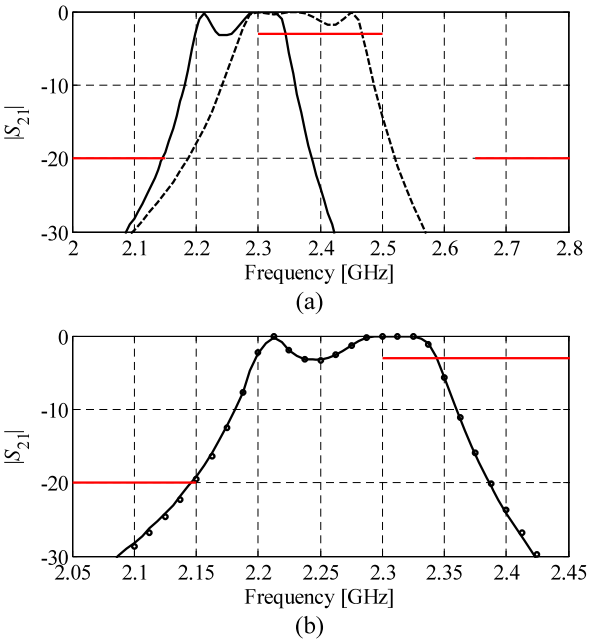

Fig. 3 Coupled microstrip bandpass filter: (**a**) responses of the fine model (*solid line*) and the coarse model (*dashed line*) at the initial design; (**b**) responses of the fine model (*solid line*) and the SM surrogate model (*circles*) at the initial design after PE. Note the excellent match between the models

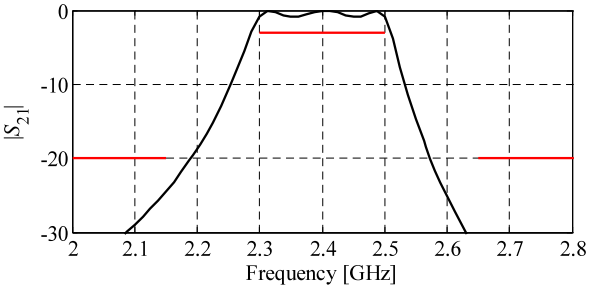

Fig. 4 Coupled microstrip bandpass filter: fine model response at the final design obtained

H_{Elem} refer to the dielectric constant (initial value 3.0) and substrate height (initial value 0.51 mm) of element *Elem*, respectively. Initial values for other parameters are zero. We take $\boldsymbol{\delta}^{(0)} = [1\ 1\ 1\ 1\ 0.3\ 0.3\ 0.3\ 0.3\ 0.4\ 0.4\ 0.4\ 0.4\ 0.02\ 0.02]^T$ (in respective units).

Figure 3(a) shows the fine and coarse model responses at the initial design. Thanks to the large number of surrogate model parameters, we obtain an excellent match to the fine model, as illustrated in Fig. 3(b). Figure 4 shows the fine model response at the final design.

Table 1 Coupled bandpass filter: optimization results

Algorithm	Specification error		Number of fine model evaluations
	Best found	Final	
Standard SM	−0.9 dB	−0.4 dB	21[a]
Trust region SM	−2.1 dB	−2.1 dB	21[b]
SM with constrained PE	−2.1 dB	−2.1 dB	12

[a]Algorithm terminated after 20 iterations without convergence

[b]Terminated after 21 fine model evaluations (good convergence pattern, but tolerance requirements not fulfilled yet)

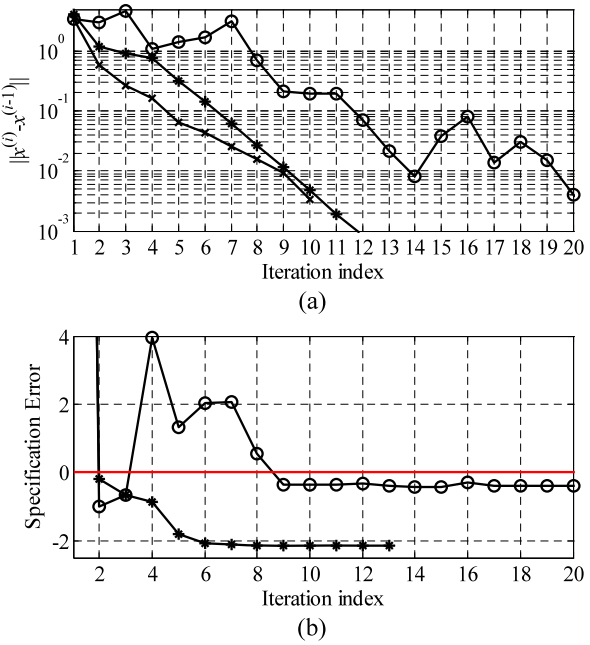

Fig. 5 Coupled microstrip bandpass filter: (**a**) convergence plot for the standard SM (o), trust region enhanced SM (×), and for the constrained algorithm (∗). Note that there is more than one fine model evaluation per iteration for the trust region algorithm (21 evaluations in total); (**b**) specification error versus iteration index for the standard SM (o) and for the constrained algorithm (∗)

Optimization results for standard and trust region enhanced SM as well as for the constrained algorithm of Sect. 3.2 are summarized in Table 1 as well as in Fig. 5. We observe that the standard algorithm exhibits features typical of SM: fast initial progress, then stagnation, as indicated by the lack of or slow convergence, and oscillation in the specification error values. On the other hand, the algorithm exhibits both a nice convergence pattern and consistent behavior with respect to specification error. The trust region convergence improves the convergence properties of the

algorithm, but at the expense of extra computational effort: any designs that do not reduce the specification error are rejected, so typically more than one fine model evaluation per iteration is required for this algorithm. The total optimization cost is almost twice as high as for the constrained algorithm.

4 Design of Antennas Using Space Mapping with Response Surface Approximation Coarse Models

In this section we deal with a specific modification of the SM algorithm that is suitable in situations when the underlying low-fidelity model is relatively expensive. This is particularly the case for antenna structures, where reliable equivalent circuit models are usually not available, and the only universal way to create a faster representation of the structure is coarse-discretization EM simulation.

4.1 Response Surface Approximation Coarse Models

As mentioned before, the coarse model is a critical component of successful SM optimization. The model should be physics-based; i.e., it should describe the same phenomena as the fine model. This ensures that the surrogate model constructed using $\boldsymbol{R}_c$ will have good prediction capability [15]. Also $\boldsymbol{R}_c$ should be computationally much cheaper than $\boldsymbol{R}_f$ so that the total costs of surrogate model optimization (2) and PE (4) problems are negligible. The preferred choice for the coarse model is therefore a circuit equivalent, e.g., one implemented in Agilent ADS [35]. Unfortunately, for many structures, particularly antennas, it is difficult to build a reliable circuit equivalent, or the circuit equivalent may be of insufficient accuracy, resulting in poor performance of the SM process.

In general, $\boldsymbol{R}_c$ can be implemented using the same EM solver as the one of the fine model by applying relaxed mesh requirements. However, the coarse-mesh model may have poor analytical properties (e.g., numerical noise, nondifferentiability and discontinuity of the response over the design variables) which make optimization of the surrogate difficult [11]. Also, it is not straightforward to find an appropriate trade-off between the model accuracy and evaluation time. The rule of thumb is that the evaluation time of $\boldsymbol{R}_c$ should be at least two orders of magnitude smaller than that of $\boldsymbol{R}_f$ in order to make the overhead of solving (2) and (4) reasonably small.

We mention that coarse mesh is not the only different feature of the coarse model compared to the fine model. Other options include: (i) a reduced number of cells in the perfectly matched layer absorbing boundary conditions as well as a reduced distance from the simulated structure to the absorbing boundary conditions, in the case of finite-volume EM simulators [36–38]; (ii) the lower order of the basis functions, in the case of finite-element and integral equation solvers [37, 38]; (iii) simplified

excitation [38, 39], e.g., the discrete source of the coarse model versus the waveguide port of the fine model; (iv) zero thickness of metallization; (v) the use of a perfect electric conductor in place of finite-conductivity metals.

In this chapter, a coarse model is built using a functional approximation of data obtained with the same EM simulator as the fine model but with a much coarser mesh. This coarse-discretization EM-based model will be denoted as $\boldsymbol{R}_{\text{cd}}$. Note that the functional approximation model would normally be set up using sampled fine model data. Here, in order to reduce the computational overhead, the surrogate is constructed using its simplified representation, $\boldsymbol{R}_{\text{cd}}$.

A variety of function approximation methods are available, including polynomial approximation [5], neural networks [40–44], kriging [5, 45, 46], multidimensional Cauchy approximation [47], or support vector regression [48]. Here, the coarse model is constructed using kriging interpolation. We made this choice not only because kriging is a reliable and popular technique [5], but also because the available Matlab kriging toolbox, DACE [49], allows us to configure kriging-based models in an efficient way. For brevity, we omit a formulation of the details of kriging. The interested reader can find them in the literature (e.g., [5] or [9]).

Response surface approximation in general (and kriging interpolation in particular) as a method of generating the coarse model for the SM algorithm has a number of advantages: (i) the resulting model is computationally cheap, smooth, and therefore, easy to optimize; (ii) there is no need for an equivalent circuit model, and, consequently, no extra simulation software is needed; the SM algorithm implementation is simpler and exploits a single EM solver; (iii) it is possible to apply SM for antenna design problems where finding reliable and fast coarse models is difficult or impossible; (iv) the initial design obtained through optimization of the coarse-mesh EM model is usually better than the initial design that could be obtained by other methods.

4.2 Design Optimization Process

The design optimization procedure can be summarized as follows (Fig. 6):

1. Take initial design $\boldsymbol{x}^{\text{init}}$;
2. Find the starting point $\boldsymbol{x}^{(0)}$ for SM algorithm by optimizing the coarse-discretization model $\boldsymbol{R}_{\text{cd}}$;
3. Allocate N base designs, $X_B = \{\boldsymbol{x}^1, \ldots, \boldsymbol{x}^N\}$;
4. Evaluate $\boldsymbol{R}_{\text{cd}}$ at each design $\boldsymbol{x}^j$, $j = 1, 2, \ldots, N$;
5. Build the coarse model $\boldsymbol{R}_c$ as a kriging interpolation of data pairs $\{(\boldsymbol{x}^j, \boldsymbol{R}_{\text{cd}}(\boldsymbol{x}^j))\}_{j=1,\ldots,N}$;
6. Set $i = 0$;
7. Evaluate the fine model $\boldsymbol{R}_f$ at $\boldsymbol{x}^{(i)}$;
8. Construct the space mapping surrogate model $\boldsymbol{R}_s^{(i)}$ as in (3) and (4);
9. Find a new design $\boldsymbol{x}^{(i+1)}$ as in (2);

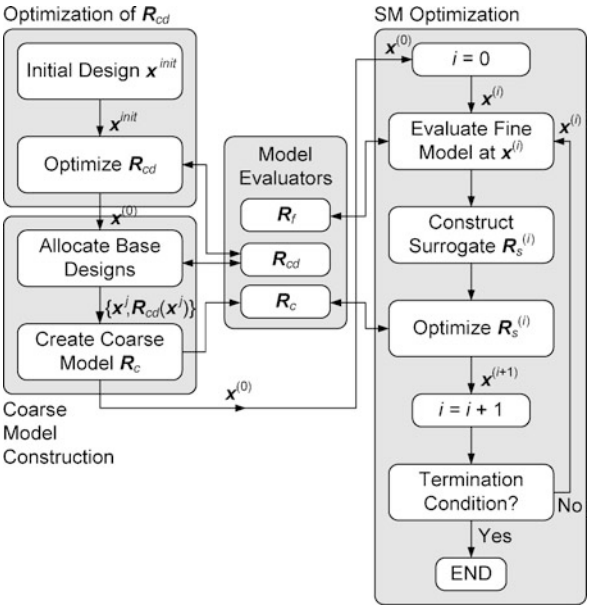

Fig. 6 Flowchart of the design optimization procedure exploiting a response-surface-approximation-based coarse model and SM as the main optimization engine [9]

10. Set $i = i + 1$;
11. If the termination condition is not satisfied go to 7;
12. END

The first phase of the design process is to find an optimized design of the coarse-discretization model. The optimum of $\boldsymbol{R}_{\text{cd}}$ is usually the best design we can get at a reasonably low computational cost. This cost can be further reduced by relaxing tolerance requirements while searching for $\boldsymbol{x}^{(0)}$: due to a limited accuracy of $\boldsymbol{R}_{\text{cd}}$ it is sufficient to find only a rough approximation of its optimum. Steps 3–5 describe the construction of the kriging-based coarse model. Steps 6–12 describe the flow of the SM algorithm. In principle, any SM surrogate model can be used except one from implicit SM, as the kriging-based coarse model normally does not inherit pre-assigned parameters from the coarse-discretization EM model. Here, the algorithm is terminated when no improvement of the fine model objective function is obtained in a given iteration. In general, the algorithm can be embedded in the trust region framework [22] for improved convergence.

The mesh density for the coarse-discretization model $\boldsymbol{R}_{\text{cd}}$ should be adjusted so that its evaluation time is substantially smaller than that of the fine model and, at the same time, its accuracy is still decent. Typically, if $\boldsymbol{R}_{\text{cd}}$ is set up so that it is 20 to 60 times faster than $\boldsymbol{R}_f$, its accuracy is acceptable for the purpose of the design procedure. The coarse model is created in the neighborhood X_N of $\boldsymbol{x}^{(0)}$, the approximate optimum of the coarse-discretization model $\boldsymbol{R}_{\text{cd}}$. The relative size of this neighborhood depends on the sensitivity of the antenna response to design variables as well

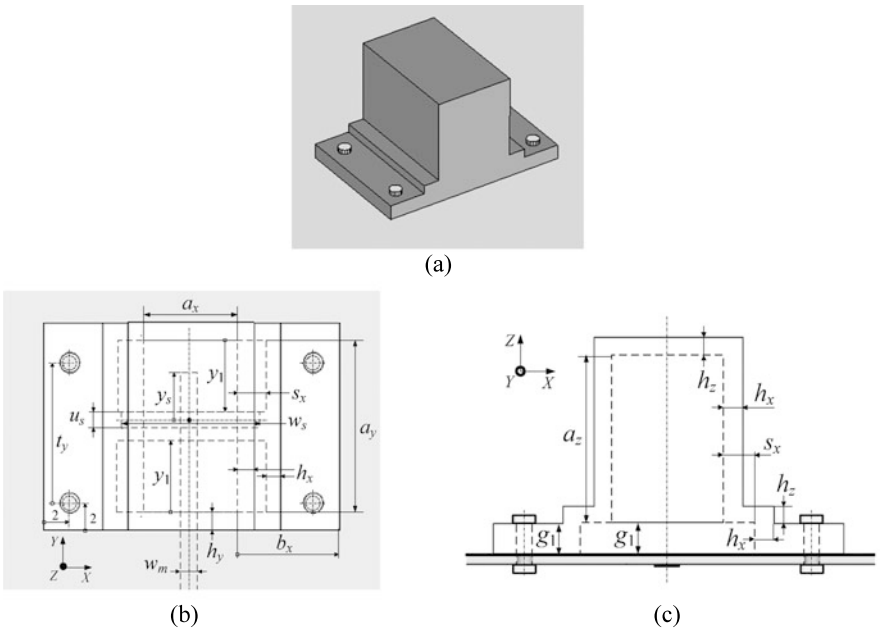

Fig. 7 DRA: (**a**) 3D view, (**b**) top view, and (**c**) front view; substrate shown transparent

as the discrepancy between the fine and coarse-discretization models, and may vary from a few to 20 percent. The number of base designs N depends on the problem dimensionality; typical values are 50 to 200. The base points should be allocated as uniformly as possible in X_N. Here, we use a modified Latin hypercube sampling [50] algorithm that gives a fairly uniform distribution of samples regardless of the number of design variables.

4.3 Design Example: Dielectric Resonator Antenna

Consider a rectangular DRA [51]; see Fig. 7 for its geometry. The DRA comprises a rectangular dielectric resonator (DR) estimated to operate at the perturbed $\text{TE}_{\delta 11}$ mode [51], supporting RO4003C [52] slabs, and polycarbonate housing. The housing is fixed to the circuit board with four through M1 bolts. The DRA is energized with a 50 Ω microstrip through a slot made in the metal ground. The substrate is 0.5 mm thick RO4003C. The design specifications are $|S_{11}| \leq -15$ dB for 5.1–5.9 GHz; also the DRA is required to have an antenna gain of better than 5 dBi for the zero zenith angle over the bandwidth of interest.

There are nine design variables: $\boldsymbol{x} = [a_x\ a_y\ a_z\ a_{y0}\ u_s\ w_s\ y_s\ g_1\ y_1]^T$, where a_x, a_y, and a_z are the dimensions of the DR, a_{y0} stands for the offset of the DR center relative to the slot center (marked by a black dot in Fig. 7(b)) in the Y-direction, u_s

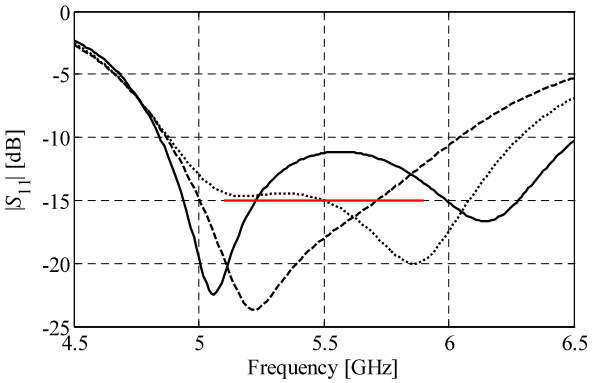

Fig. 8 DRA, $|S_{11}|$ versus frequency: fine model $\boldsymbol{R}_f$ at the initial design (- - -), optimized coarse-discretization model $\boldsymbol{R}_{\text{cd}}$ ($\cdot\ \cdot\ \cdot$), and $\boldsymbol{R}_f$ at the optimum of $\boldsymbol{R}_{\text{cd}}$ ($-$)

and w_s are the slot dimensions, y_s is the length of the microstrip stub, and g_1 and y_1 are the slab dimensions. The relative permittivity and loss tangent of the DR are 10 and 1e-4, respectively, at 6.5 GHz.

The width of the microstrip signal trace is 1.15 mm. Metallization of the trace and ground is done with 50 μm copper. The relative permittivity and loss tangent of the polycarbonate housing are 2.8 and 0.01 at 6.5 GHz, respectively. DRA models are defined with the CST MWS [39], and the built-in single-pole Debye model is used for all dielectrics to describe their dispersion properties. Other dimensions are fixed as follows: $h_x = h_y = h_z = 1$, $b_x = 7.5$, $s_x = 2$, and $t_y = a_y - a_{y0} - 1$, all in millimeters.

The initial design is $\boldsymbol{x}^{\text{in}} = [8.000\ 14.000\ 9.000\ 0\ 1.750\ 10.000\ 3.000\ 1.500\ 6.000]^T$ mm. The fine (1,099,490 mesh cells at $\boldsymbol{x}^{\text{in}}$) and coarse-discretization (26,796 mesh cells at $\boldsymbol{x}^{\text{in}}$) antenna models are evaluated with CST MWS transient solver in 2,175 and 42 s, respectively.

A coarse-discretization model optimum is $\boldsymbol{x}^{(0)} = [7.444\ 13.556\ 9.167\ 0.250\ 1.750\ 10.500\ 2.500\ 1.500\ 6.000]^T$ mm. Figure 8 shows the fine model reflection response at the initial design as well as that of the fine and coarse-discretization model $\boldsymbol{R}_{\text{cd}}$ at $\boldsymbol{x}^{(0)}$. The kriging coarse model is set up using 200 samples of $\boldsymbol{R}_{\text{cd}}$ allocated in the vicinity of $\boldsymbol{x}^{(0)}$ of size $[0.5\ 0.5\ 0.5\ 0.25\ 0.5\ 0.25\ 0.25\ 0.25\ 0.5]^T$ mm.

The final design, $\boldsymbol{x}^{(4)} = [7.556\ 13.278\ 9.630\ 0.472\ 1.287\ 10.593\ 2.667\ 1.722\ 6.482]^T$ mm, is obtained after four SM iterations; its reflection response is shown in Fig. 9. The far-field response of the final design is shown in Fig. 10. For the bandwidth of interest, the peak gain is above 5 dBi, and the back radiation level is below -14 dB (relative to the maximum). All responses shown include the effect of the 25 mm input microstrip. The surrogate model used by the optimization algorithm exploited input and output SM of the form $\boldsymbol{R}_s(\boldsymbol{x}) = \boldsymbol{R}_c(\boldsymbol{x} + \boldsymbol{c}) + \boldsymbol{d}$. The optimization costs are summarized in Table 2. The total design time corresponds to about 11 evaluations of the fine model.

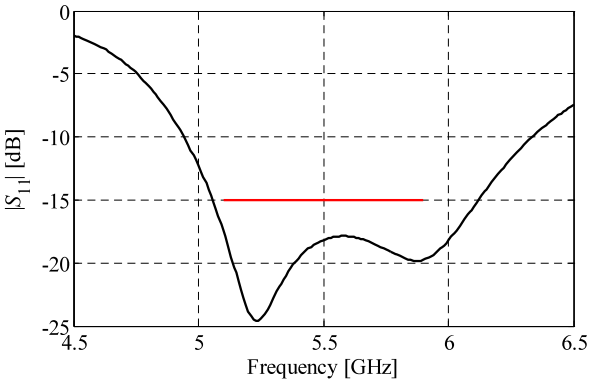

Fig. 9 DRA, $|S_{11}|$ versus frequency: $\boldsymbol{R}_f$ at the final design

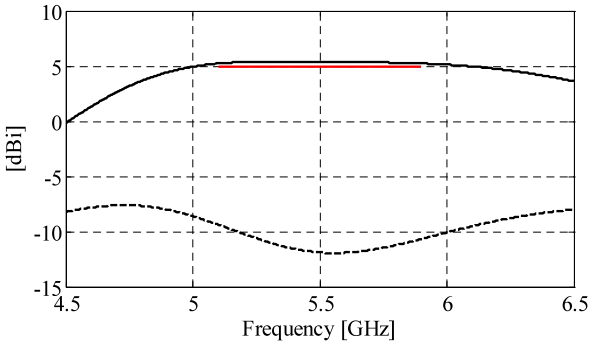

Fig. 10 DRA, realized gain versus frequency: (—) is for the zero zenith angle ($\theta = 0^0$); (- - -) is back radiation for $\theta = 180°$. Here, only θ-polarization ($\phi = 90°$) contributes to the gain for the listed directions

Table 2 DRA: optimization cost

Algorithm component	Number of model evaluations	CPU time	
		Absolute	Relative to $\boldsymbol{R}_f$
Optimization of $\boldsymbol{R}_{\text{cd}}$	$150 \times \boldsymbol{R}_{\text{cd}}$	105 min	2.9
Setting up $\boldsymbol{R}_c$	$200 \times \boldsymbol{R}_{\text{cd}}$	140 min	3.9
Evaluation of $\boldsymbol{R}_f$	$4 \times \boldsymbol{R}_f$	145 min	4.0
Total cost	N/A	390 min	10.8

5 Space Mapping with Adjoint Sensitivity

In this section, we discuss the use of adjoint sensitivity [53] to enhance conventional SM optimization algorithms. More specifically, adjoint sensitivity is exploited to:

(i) speed up the surrogate model optimization process (2), (ii) speed up the PE process (4), and (iii) improve the matching between the surrogate and the high-fidelity model. Due to (i) and (ii), both PE and surrogate model optimization can be performed using a small number of low-fidelity model evaluations, which allows us to utilize coarse-discretization EM coarse models. This widens SM applications as well as improving SM performance, as low-fidelity SM models are normally quite accurate. Adjoint sensitivities are also used to match both the responses and first-order derivatives of the surrogate and the high-fidelity model, which improves the performance and convergence properties of the SM algorithm [54]. An illustrative example is provided.

5.1 Low-Fidelity and Surrogate Models

SM with adjoint sensitivity follows the generic SM scheme (2). As usual, the surrogate model is constructed using the underlying low-fidelity (or coarse) model $\boldsymbol{R}_c$, which is a simplified representation of the high-fidelity one. Here, we focus on coarse-discretization EM models, as they allow us to extend the applicability of SM to all conceivable microwave structures. Coarse-discretization EM models are typically accurate but relatively expensive; therefore, the SM surrogate exploited here is based on input and output SM [21] of the form:

$$\boldsymbol{R}_s^{(i)}(\boldsymbol{x}) = \boldsymbol{R}_c\big(\boldsymbol{x} + \boldsymbol{c}^{(i)}\big) + \boldsymbol{d}^{(i)} + \boldsymbol{E}^{(i)}\big(\boldsymbol{x} - \boldsymbol{x}^{(i)}\big). \tag{9}$$

Here, only the input SM vector $\boldsymbol{c}^{(i)}$ is obtained through the nonlinear PE process

$$\boldsymbol{c}^{(i)} = \arg\min_{\boldsymbol{c}} \big\| \boldsymbol{R}_f\big(\boldsymbol{x}^{(i)}\big) - \boldsymbol{R}_c\big(\boldsymbol{x}^{(i)} + \boldsymbol{c}\big) \big\|. \tag{10}$$

Output SM parameters are calculated as

$$\boldsymbol{d}^{(i)} = \boldsymbol{R}_f\big(\boldsymbol{x}^{(i)}\big) - \boldsymbol{R}_c\big(\boldsymbol{x}^{(i)} + \boldsymbol{c}^{(i)}\big) \tag{11}$$

and

$$\boldsymbol{E}^{(i)} = \boldsymbol{J}_{\boldsymbol{R}_f}\big(\boldsymbol{x}^{(i)}\big) - \boldsymbol{J}_{\boldsymbol{R}_c}\big(\boldsymbol{x}^{(i)} + \boldsymbol{c}^{(i)}\big), \tag{12}$$

where $\boldsymbol{J}$ denotes the Jacobian of the respective model obtained using adjoint sensitivities. Formulation (2)–(5) ensures zero- and first-order consistency [55] between the surrogate and the fine model, i.e., $\boldsymbol{R}_s^{(i)}(\boldsymbol{x}^{(i)}) = \boldsymbol{R}_f(\boldsymbol{x}^{(i)})$ and $\boldsymbol{J}_{\boldsymbol{R}_s^{(i)}}(\boldsymbol{x}^{(i)}) = \boldsymbol{J}_{\boldsymbol{R}_f}(\boldsymbol{x}^{(i)})$, which substantially improves the ability of the SM algorithm to quickly locate the high-fidelity model optimum [55]. Here, the algorithm (2) is embedded in the trust region framework [30]; i.e., we have $\boldsymbol{x}^{(i+1)} = \arg\min\{\|\boldsymbol{x} - \boldsymbol{x}^{(i)}\| \le \delta^{(i)} : U(\boldsymbol{R}_s^{(i)}(\boldsymbol{x}))\}$, where the trust region radius $\delta^{(i)}$ is updated using classical rules [30]. Assuming first-order consistency and smoothness of $\boldsymbol{R}_s^{(i)}(\boldsymbol{x})$, this ensures convergence to the local $\boldsymbol{R}_f$ optimum.

5.2 Fast Parameter Extraction and Surrogate Optimization Using Adjoint Sensitivities

To speed up the PE process (4), we exploit adjoint sensitivities. We use a simple trust-region-based [22] algorithm, where the approximate solution $\boldsymbol{c}^{(i.k+1)}$ of $\boldsymbol{c}^{(i)}$ is found as (k is the iteration index for PE process (13))

$$\boldsymbol{c}^{(i.k+1)} = \arg \min_{\|\boldsymbol{c}-\boldsymbol{c}^{(i.k)}\| \le \delta_{\mathrm{PE}}^{(k)}} \left\| \boldsymbol{R}_f\left(\boldsymbol{x}^{(i)}\right) - \boldsymbol{L}_{c.c}^{(i.k)}(\boldsymbol{c}) \right\|, \tag{13}$$

where $\boldsymbol{L}_{c.c}^{(i.k)}(\boldsymbol{c}) = \boldsymbol{R}_c(\boldsymbol{x}^{(i)} + \boldsymbol{c}^{(i.k)}) + \boldsymbol{J}_{\boldsymbol{R}_c}(\boldsymbol{x}^{(i)} + \boldsymbol{c}^{(i.k)}) \cdot (\boldsymbol{c} - \boldsymbol{c}^{(i.k)})$ is a linear approximation of $\boldsymbol{R}_c(\boldsymbol{x}^{(i)} + \boldsymbol{c})$ at $\boldsymbol{c}^{(i.k)}$. The trust region radius $\delta_{\mathrm{PE}}^{(k)}$ is updated according to standard rules [22]. PE is terminated upon convergence or exceeding the maximum number of coarse model evaluations (here, the limit is set to 5, which is sufficient when using adjoint sensitivity).

Adjoint sensitivities are also utilized to lower the cost of surrogate model optimization. Similarly to (13), we use a trust-region-based algorithm that produces a sequence of approximations $\boldsymbol{x}^{(i+1.k)}$ of the solution $\boldsymbol{x}^{(i+1)}$ to (2) as follows (k is the iteration index for surrogate model optimization process (14)):

$$\boldsymbol{x}^{(i+1.k+1)} = \arg \min_{\|\boldsymbol{x}-\boldsymbol{x}^{(i+1.k)}\| \le \delta_{\mathrm{SO}}^{(k)}} U\left(\boldsymbol{L}_{c.x}^{(i.k)}(\boldsymbol{x})\right), \tag{14}$$

where $\boldsymbol{L}_{c.x}^{(i.k)}(\boldsymbol{x}) = \boldsymbol{R}_s^{(i)}(\boldsymbol{x}^{(i+1.k)} + \boldsymbol{c}^{(i)}) + \boldsymbol{J}_{\boldsymbol{R}_s^{(i)}}(\boldsymbol{x}^{(i+1.k)} + \boldsymbol{c}^{(i)}) \cdot (\boldsymbol{x} - \boldsymbol{x}^{(i+1.k)})$ is a linear approximation of $\boldsymbol{R}_s^{(i)}(\boldsymbol{x} + \boldsymbol{c}^{(i)})$ at $\boldsymbol{x}^{(i+1.k)}$. The trust region radius $\delta_{\mathrm{SO}}^{(k)}$ is updated according to standard rules [54]. Typically, due to adjoint sensitivities, surrogate model optimization requires only a few evaluations of the coarse model $\boldsymbol{R}_c$. Note that the sensitivities of the surrogate model can be calculated using the sensitivities of both $\boldsymbol{R}_f$ and $\boldsymbol{R}_c$ as follows: $\boldsymbol{J}_{\boldsymbol{R}_s^{(i)}}(\boldsymbol{x} + \boldsymbol{c}^{(i)}) = \boldsymbol{J}_{\boldsymbol{R}_c}(\boldsymbol{x} + \boldsymbol{c}^{(i)}) + [\boldsymbol{J}_{\boldsymbol{R}_f}(\boldsymbol{x}^{(i)}) - \boldsymbol{J}_{\boldsymbol{R}_c}(\boldsymbol{x}^{(i)} + \boldsymbol{c}^{(i)})]$.

5.3 Design Example: Dielectric Resonator Filter

Consider the dielectric resonator filter [56] shown in Fig. 11. The design variables are $\boldsymbol{x} = [u_1\ u_2\ u_3\ v_1\ v_2]^T$ mm, and the relative permittivity of the dielectric resonators (DR) is $\varepsilon_{r1} = 38$. The relative permittivity of the DR supports and the coax filling is $\varepsilon_{r2} = 2.1$. The materials are considered lossless. Here $h_3 = h_4 = h_5 = 1$ mm, $r_3 = r_2$ (the inner radius of the DR), and $r_4 = r_2 + 1$ mm, and $\rho_1 = 2.05$ mm. Other dimensions are fixed as in [56].

The filter models are simulated by the CST MWS transient solver [39]. The coarse-discretization model $\boldsymbol{R}_{\mathrm{cd}}$ comprises 38,220 hexahedral cells and runs for 1 min, and the fine model $\boldsymbol{R}_f$ comprises 333,558 cells and runs for 28 min, both at the initial design which is $\boldsymbol{x}^{(\mathrm{init})} = [8\ 12\ 25\ 25\ -10]^T$ mm. The design specifications are $|S_{21}| \ge -0.75$ dB for 4.52 GHz $\le \omega \le$ 4.54 GHz, and $|S_{21}| \le -20$ dB for 4.4 GHz $\le \omega \le$ 4.47 GHz and 4.59 GHz $\le \omega \le$ 4.63 GHz.

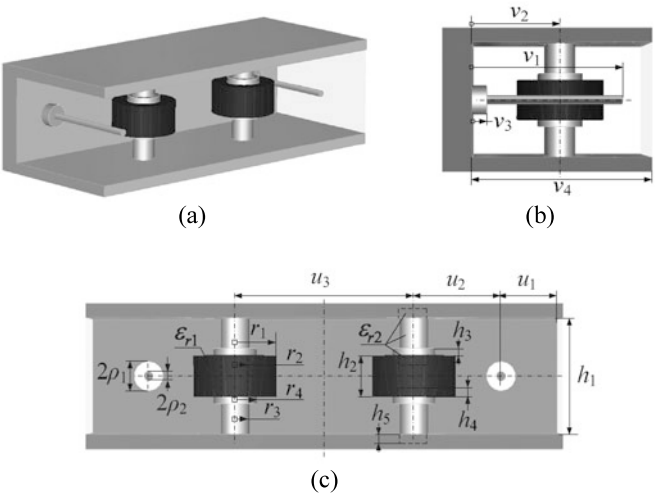

Fig. 11 Dielectric resonator filter [56]: (**a**) 3D view, (**b**) side view, and (**b**) front view. Front and side metal walls of the waveguide section are shown transparent

Table 3 Dielectric resonator filter: optimization results

Algorithm component	Number of model evaluations[a]	CPU time	
		Absolute [min]	Relative to $\boldsymbol{R}_f$
Evaluation of $\boldsymbol{R}_c$	80	80	2.9
Evaluation of $\boldsymbol{R}_f$	11	308	11
Total cost[a]	N/A	398	**13.9**

[a]Excludes $\boldsymbol{R}_f$ evaluation at the initial design

The filter was optimized using the algorithm of Sects. 5.1 and 5.2. Figure 12(a) shows the responses of $\boldsymbol{R}_f$ and $\boldsymbol{R}_c$ at $\boldsymbol{x}^{\text{init}}$. Figure 12(b) shows the response of the fine model at the final design $\boldsymbol{x}^{(*)} = [7.28\ 11.06\ 24.81\ 26.00\ -11.07]^T$ mm obtained after ten SM iterations. Table 3 summarizes the total optimization cost. Note that using adjoint sensitivities allows us to greatly reduce the number of both fine and coarse model evaluations in the design process. The average cost of the PE and surrogate optimization processes is only about 5 evaluations of $\boldsymbol{R}_c$. The evolution of the specification error is shown in Fig. 13.

6 Conclusion

In this chapter, a number of design examples concerning various microwave components have been presented, including microstrip filters and planar antennas, as well as transition structures. In all cases, the surrogate-based techniques presented

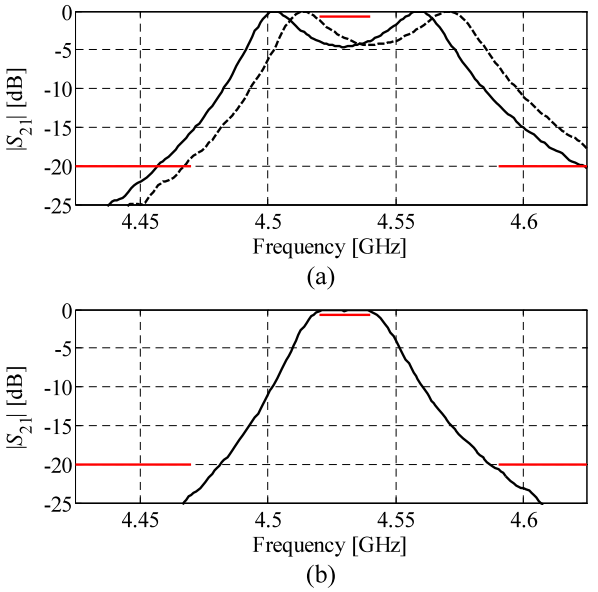

Fig. 12 Dielectric resonator filter: (**a**) responses of $\boldsymbol{R}_f$ (—) and $\boldsymbol{R}_c$ (- - -) at the initial design $\boldsymbol{x}^{\text{init}}$, (**b**) response of $\boldsymbol{R}_f$ (—) at the final design

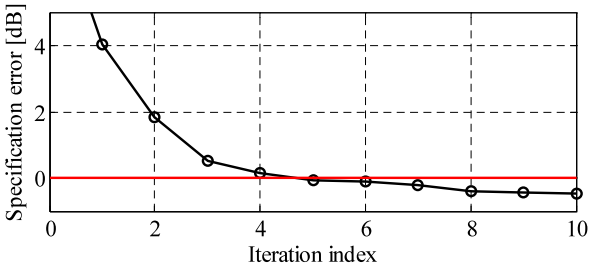

Fig. 13 Dielectric resonator filter: minimax specification error versus SM iteration index

here have been employed as optimization engines. The results presented here indicate that the surrogate-based optimization methods make the simulation-driven microwave design feasible and efficient, in terms of both the quality of the final design and the computational cost. In most cases, the design cost corresponds to a few high-fidelity electromagnetic simulations of the microwave structure under consideration, typically comparable to the number of design variables. While this kind of performance is definitely appealing, improved robustness and reliability as well as availability through commercial software packages are needed to make the surrogate-based techniques widely accepted by the microwave engineering community. Therefore, a substantial research effort in this area is expected in the years to come.